

\*Work supported by the National Science Foundation.

†Work supported in part by the U. S. Atomic Energy Commission under AEC contract No. At(30-1)-2098.

<sup>1</sup>D. F. Jackson, Phys. Letters 32B, 233 (1970); C. G. Morgan and D. F. Jackson, Phys. Rev. 188, 1758 (1969); D. F. Jackson and V. K. Kumbhavi, *ibid.* 178, 1 26 (1969).

<sup>2</sup>A. M. Bernstein and W. A. Seidler, II, Phys. Letters 34B, 569 (1971); 39B, 583 (1972).

<sup>3</sup>I. Reichstein and Y. C. Tang, Nucl. Phys. A139, 144 (1969).

<sup>4</sup>A. M. Bernstein, in *Advances in Nuclear Physics*, edited by M. Baranger and E. Vogt (Plenum Press, New York, 1969), Vol. 3.

<sup>5</sup>A. M. Bernstein and W. A. Seidler, II, to be published.

<sup>6</sup>C. J. Batty, E. Friedman, and D. F. Jackson, Nucl. Phys. A175, 1 (1971).

<sup>7</sup>G. M. Lerner, J. C. Hiebert, and L. Rutledge, Bull. Am. Phys. Soc. 17, 536 (1972).

<sup>8</sup>B. Tatischeff, I. Brissaud, and L. Bimbot, Phys. Rev. C 5, 234 (1972).

<sup>9</sup>W. A. Seidler, II, Ph.D. thesis, Massachusetts Institute of Technology, 1972 (unpublished).

<sup>10</sup>R. Hofstadter, F. Bumiller, and M. R. Yearian, Rev. Mod. Phys. 30, 482 (1958).

<sup>11</sup>R. F. Frosch *et al.*, Phys. Rev. 174, 1380 (1968).

<sup>12</sup>B. Fernandez and J. S. Blair, Phys. Rev. C 1, 523 (1969).

<sup>13</sup>G. Hauser *et al.*, Nucl. Phys. A128, 81 (1969); G. Schatz, private communication.

<sup>14</sup>J. W. Negele, Phys. Rev. C 1, 1260 (1970).

<sup>15</sup>W. T. H. van Oers, Phys. Rev. C 3, 1550 (1971).

<sup>16</sup>F. G. Perey and B. Buck, Nucl. Phys. 32, 353 (1962).

PHYSICAL REVIEW C

VOLUME 6, NUMBER 4

OCTOBER 1972

## Study of ( $^3\text{He}, t$ ) Reactions at 70 MeV to Isobaric Analog States of $^{50}\text{Cr}$ , $^{62}\text{Ni}$ , and $^{90}\text{Zr}$ †

R. A. Hinrichs and D. L. Show

*Cyclotron Laboratory, Michigan State University, East Lansing, Michigan 48823*

(Received 24 April 1972)

The analysis of ( $^3\text{He}, t$ ) reactions at 70 MeV to isobaric analog ground states of  $^{50}\text{Cr}$ ,  $^{62}\text{Ni}$ , and  $^{90}\text{Zr}$  have shown an energy dependence in the extracted isospin-dependent interaction strengths consistent with results at lower energies; the interaction strengths are approximately 50% smaller than at lower bombarding energies. The shapes of the form factors in a macroscopic analysis are nuclei-dependent. A mass-three optical potential with a real strength of about 110 MeV and a volume imaginary term is strongly preferred in the ( $^3\text{He}, t$ ) calculations.

### I. INTRODUCTION

Charge-exchange reactions to isobaric analog states (IAS) of target ground states have been studied quite extensively in recent years with both ( $p, n$ )<sup>1,2</sup> and ( $^3\text{He}, t$ )<sup>3-6</sup> reactions at a variety of bombarding energies. The analysis of the differential cross sections for such reactions primarily has used the distorted-wave Born approximation (DWBA) in a macroscopic (generalized optical-potential) or microscopic (nucleon-nucleon interaction) framework, and has yielded information on the strength and form of the isospin-dependent interaction. Recent studies by Fadner, Kraushaar, and Hayakawa<sup>6</sup> of ( $^3\text{He}, t$ ) transitions to IAS in several nuclei at bombarding energies between 21.4 and 37.5 MeV have shown a marked energy dependence in the extracted strength of this isospin interaction and a variation in the extracted shapes of the isospin term (for the macroscopic analysis) for different nuclei. We have extended the study of ( $^3\text{He}, t$ ) reactions to 70 MeV (the high-

est reported bombarding energy has been 50 MeV<sup>7</sup>) by examining transitions to IAS of the ground states of  $^{50}\text{Cr}$ ,  $^{62}\text{Ni}$ , and  $^{90}\text{Zr}$  to provide more information on the energy dependence of the charge-exchange interaction.

### II. EXPERIMENTAL PROCEDURE AND RESULTS

The reactions  $^{50}\text{Cr}$ ,  $^{62}\text{Ni}$ ,  $^{90}\text{Zr}(^3\text{He}, t)$  were studied at a bombarding energy of 70 MeV using  $^3\text{He}$  ions accelerated in the Michigan State University sector-focused cyclotron. The experiment was conducted in a 40-in. scattering chamber with the tritons detected in a 1-cm stack of three Si(Li) detectors. A  $\Delta E$ - $E$  particle identification program was used in conjunction with the Sigma-7 computer. An over-all resolution of 150 keV was obtained, which was detector limited. The targets were all 1-mg/cm<sup>2</sup> rolled foils. An energy spectrum for the reaction  $^{62}\text{Ni}(^3\text{He}, t)^{62}\text{Cu}$  is shown in Fig. 1. At all angles the  $0^+$  IAS was populated

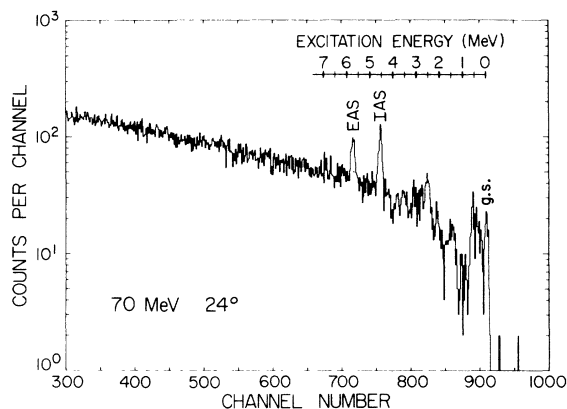


FIG. 1. Energy spectrum for the reaction  $^{62}\text{Ni}({}^3\text{He}, t)-^{62}\text{Cu}$  at  $24^\circ$ . The isobaric analogs of the ground state (IAS) and first excited state (EAS) of  $^{62}\text{Ni}$  are noted.

significantly above the continuum, although the  $2^+$  excited-state analog was not always observed and will not be discussed further. The excitation energies of the analog states are 0.0 MeV in  $^{50}\text{Mn}$ , 4.55 MeV in  $^{62}\text{Cu}$ , and 5.14 MeV in  $^{90}\text{Nb}$ . The experimental angular distributions for the three reactions are shown in Fig. 2. The data are quite similar for each nucleus and are characterized by small cross sections and strong oscillations.

### III. ANALYSIS

DWBA calculations were carried out with the computer code DWUCK<sup>8</sup> for both microscopic and macroscopic formulations.

#### A. Optical-Model Parameters

To be as general as possible, several different sets of  ${}^3\text{He}$  and  $t$  optical-model (OM) parameters taken from several sources were used in the calculations. These are listed in Table I for  $^{62}\text{Ni}$  at 70 MeV. Except in the case of the Becchetti-Greenlees parameters<sup>9</sup> (Set IV) for mass-three projectiles, the same parameters were tried for both the  ${}^3\text{He}$  and triton channels. The Becchetti-Greenlees set was established in the region  $E < 40$  MeV,  $A > 40$ , but their energy dependence was extended to 70 MeV. The somewhat standard OM

parameters of Gibson *et al.*<sup>10</sup> (Set I) have been found to possess very little dependence upon the target mass or bombarding energy, at least for energies below 43 MeV; an analysis of 70-MeV elastic scattering data<sup>11</sup> has confirmed this conclusion for higher energies. The parameters of Set II (Fulmer<sup>12</sup>) were those found from an analysis of 71-MeV  $^{62}\text{Ni}$  elastic scattering, and the parameters of Set III (MSU) are taken from an analysis of 70-MeV  ${}^3\text{He}$  elastic scattering on  $^{50}\text{Ti}$  and  $^{51}\text{V}$ .<sup>11</sup> In this last study, several families of OM parameters which fit this data were generated starting from the geometry of Set I. More will be said concerning these families later.

#### B. Macroscopic Calculations

With the introduction of an asymmetry term  $U_1(r)$  into the projectile-nucleus optical potential, giving a form

$$U = U_0(r) + U_1(r)\bar{t} \cdot \bar{\tau}/A,$$

where  $\bar{t}$  and  $\bar{\tau}$  are the isospin operators for the projectile and target nucleus, respectively, one can account for the charge-exchange process to isobaric analog ground states by the off-diagonal part of the  $\bar{t} \cdot \bar{\tau}$  matrix. In the formalism of the DWBA, the transition amplitude for "quasielastic" scattering to the IAS is

$$T = \frac{1}{A} \left( \frac{N-Z}{2} \right)^{1/2} \int d\vec{r} X_t^{(-)*}(\vec{k}_t, \vec{r}) U_1(\vec{r}) X_h^{(+)}(\vec{k}_h, \vec{r}), \quad (1)$$

where the  $X(k, r)$  are the distorted waves of the  ${}^3\text{He}$  and  $t$  channels, and the interaction potential  $U_1(r)$  is the same as the term in the above generalized optical potential. In analyses of  $({}^3\text{He}, t)$  data to IAS, a complex form for  $U_1(r)$  has been found to yield the best description of the data.<sup>3</sup> The isospin-dependent potential used in our macroscopic calculations is

$$U_1 = Vf(x) + i4W \frac{d}{dx'} f(x'),$$

where

$$x = \frac{r - R_0}{a} \quad \text{and} \quad f(x) = \frac{1}{1 + e^x}. \quad (2)$$

TABLE I. OM parameters; 70 MeV,  $^{62}\text{Ni}$ .

Set	$V$	$r_0$	$a$	$W_v$	$W_D$	$r_I$	$a_I$	Reference
I	170.6	1.14	0.712	18.5	...	1.6	0.829	Gibson (Ref. 10)
II	126.5	1.12	0.837	...	20.4	1.26	0.841	Fulmer (Ref. 12)
III	114.2	1.14	0.842	18.4	...	1.62	0.793	MSU (Ref. 11)
IV	${}^3\text{He}$ : 145	1.20	0.72	22.9	...	1.40	0.88	Becchetti-Greenlees (Ref. 9)
	$t$ : 152.4	1.20	0.72	12.3	...	1.40	0.84	

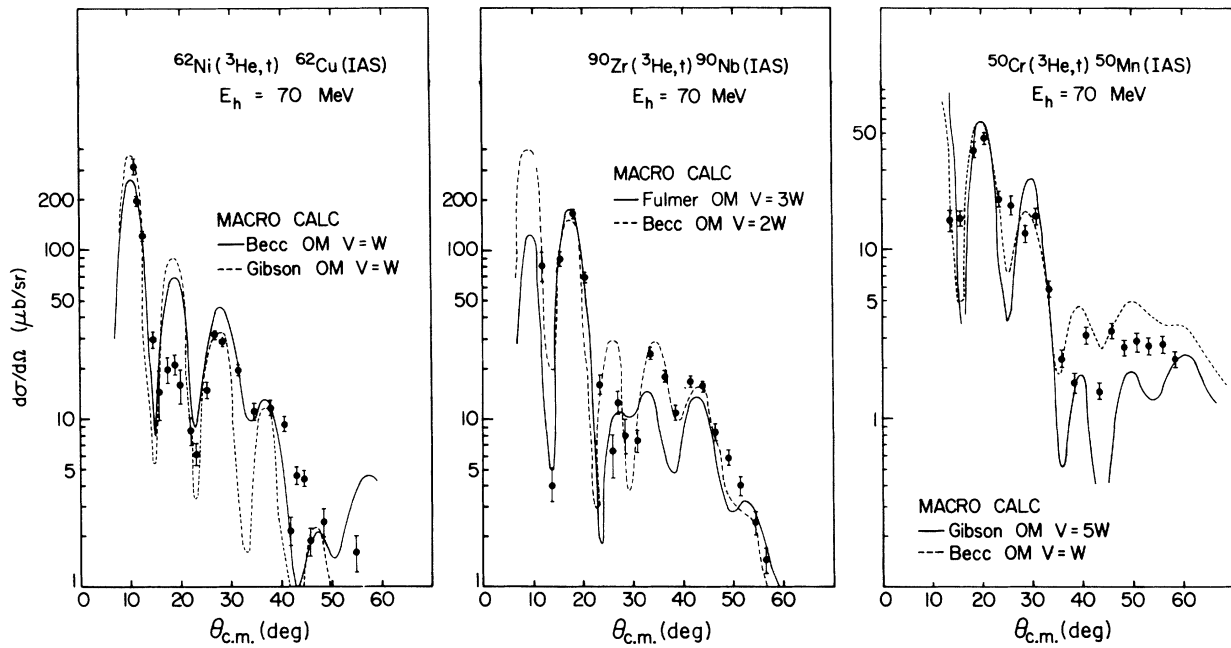


FIG. 2. Angular distributions for ( ${}^3\text{He}, t$ ) reactions at 70 MeV to the isobaric analogs of the ground states of  ${}^{62}\text{Ni}$ ,  ${}^{90}\text{Zr}$ , and  ${}^{50}\text{Cr}$ . The curves shown are DWBA calculations with a complex macroscopic form factor (with noted relative amounts of real and imaginary strengths) for the OM parameter sets of Table I.

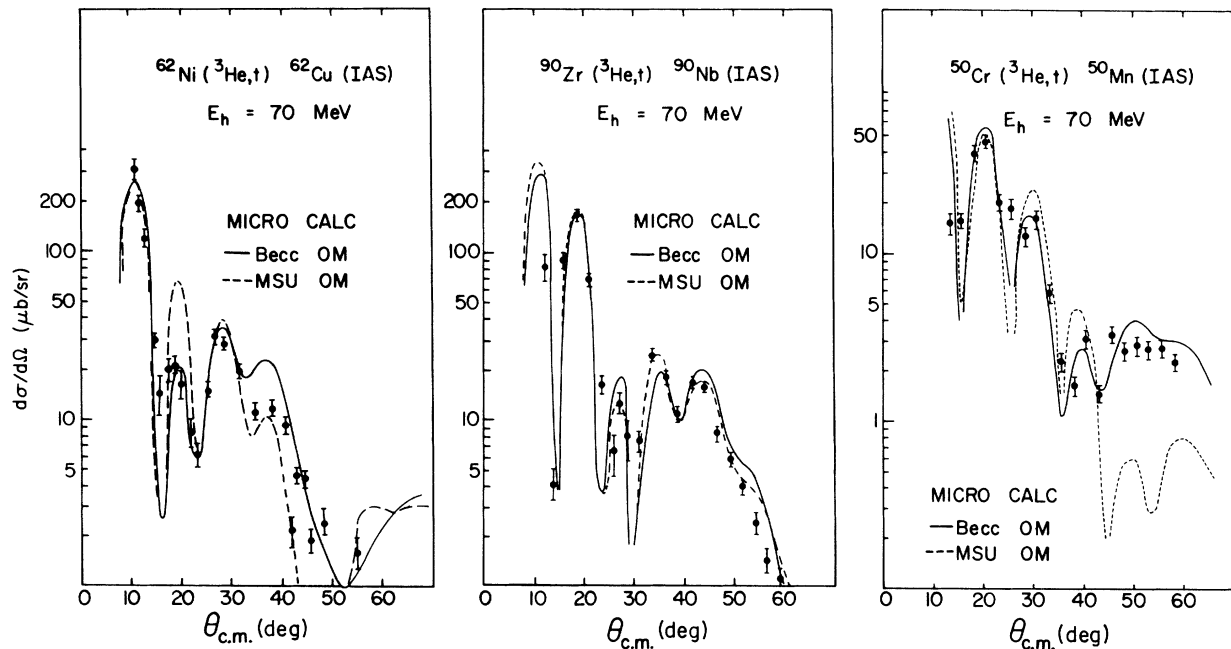


FIG. 3. Angular distributions for ( ${}^3\text{He}, t$ ) reactions at 70 MeV to the isobaric analogs of the ground states of  ${}^{62}\text{Ni}$ ,  ${}^{90}\text{Zr}$ , and  ${}^{50}\text{Cr}$ . The curves shown are microscopic DWBA calculations (normalized to the data) with simple shell-model wave functions and a Yukawa force of range 1.0 fm.

TABLE II. OM parameters;  $^{51}\text{V} + ^3\text{He}$ , 70 MeV.

Set	$V$	$r_0$	$a$	$W_v$	$W_D$	$r_I$	$a_I$	$X^2/N$
A	114.2	1.14	0.842	18.4	...	1.62	0.793	43
B	182.2	1.14	0.702	37.5	...	1.21	1.16	88
C	120.1	1.14	0.816	...	18.6	1.28	0.805	16
D	180.8	1.14	0.710	...	25.7	1.03	0.980	71

The geometry for this potential was chosen to be equal to the geometry of the real and imaginary parts of the optical potential for  $^3\text{He}$ . The imaginary part of this asymmetry term is the dominant term in the matrix element (due to its larger radius), with the real term mainly affecting the shape of the angular distributions at backward angles. In our calculations the relative strengths of the real to imaginary terms in the interaction potential or form factor were varied to provide the best possible fit for the OM set being used. Only in a few cases was it necessary to modify the geometry of the imaginary term (primarily the radius  $r_I$ ) to yield a reasonable fit to the data. In general an

increase in the relative strength of the real term  $V$  produced an increase in the differential cross section at angles of  $35\text{--}50^\circ$ , but with only negligible magnitude changes at the forward-angle maxima. In the distorted-wave channels for all calculations performed only the triton potential was varied if necessary to achieve a better fit; a larger imaginary radius or increased imaginary strength  $W_v$  tended to introduce more structure in the angular distributions, especially at backward angles, and lower the backward-angle maxima relative to those at forward angles.

Figure 2 shows some macroscopic calculations for the  $^{62}\text{Ni}$ ,  $^{90}\text{Zr}$ , and  $^{50}\text{Cr}(^3\text{He}, t)$  reactions. In general the OM parameters of Set IV provided the best theoretical fits to the data. However with appropriate variations in the shape of the form factor, fair fits were obtained for each of the OM sets listed in Table I. These will be tabulated in Sec. IV, Table III. For example for  $^{62}\text{Ni}$ , OM Set II could only provide a fit with a 20% increase in the radius of the imaginary term of the asymmetry potential and with a relative strength of  $V/W=5$ . In all cases for  $^{62}\text{Ni}$ , the second weak maximum could not be fitted, while there was difficulty with the backward-angle data of  $^{50}\text{Cr}$ .

The shapes of the form factors, as characterized by the ratio of the strength of the real term to the strength of the imaginary surface-peaked term in Eq. (2) vary over the three nuclei considered. This ratio of  $V/W$  is 1:9:2.7 for  $^{62}\text{Ni}$ ,  $^{90}\text{Zr}$ ,  $^{50}\text{Cr}$ , and OM Set I. (The data of Fadner *et al.*<sup>6</sup> at 37.5 MeV was continually reanalyzed to check if the same form factor used at 70 MeV still gave good fits at the lower energy. Fits to the 70-MeV data were more sensitive to the ratio of  $V/W$ .) This ratio, however, is quite sensitive to the OM parameters, and for Set IV  $V/W$  is 1:2:1 for  $^{62}\text{Ni}$ ,  $^{90}\text{Zr}$ ,  $^{50}\text{Cr}$ .

### C. Microscopic Calculations

DWBA calculations with an effective two-body interaction between the projectile and target nucleons of Yukawa form and range 1.0 F were carried out for these transitions. Shell-model wave functions for the analog states were taken as  $(f_{5/2})^2$  for  $^{62}\text{Cu}$ ,  $(g_{9/2})^2$  for  $^{90}\text{Nb}$ , and  $(f_{7/2})^2$  for

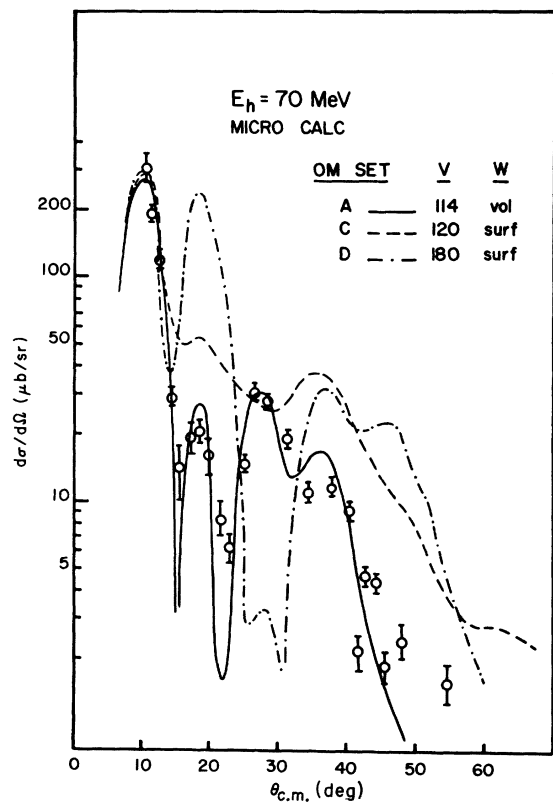


FIG. 4. Angular distributions for the reaction  $^{62}\text{Ni}-(^3\text{He}, t)^{62}\text{Cu}$  (IAS). The curves shown are DWBA calculations (normalized at the first maximum) with a microscopic form factor (Yukawa form, range 1.0 fm) with different types of OM potentials as listed in Table II.

$^{50}\text{Mn}$ . More complicated wave functions for  $^{62}\text{Cu}$  and  $^{90}\text{Nb}$  had very little effect upon the calculated angular-distribution shapes. (These wave functions were calculated in a Woods-Saxon well of geometry  $r_0=1.25$  fm,  $a=0.65$  fm; a more recently used geometry of  $r_0=1.17$  fm,  $a=0.75$  fm produced a change of only 8% in the cross section.) In general the microscopic calculations were more sensitive to the OM parameters, with only certain sets giving any fit at all. Figure 3 shows calculations for  $^{62}\text{Ni}$ ,  $^{90}\text{Zr}$ , and  $^{50}\text{Cr}$  in a microscopic formulation with OM Sets III and IV. The fits are pretty good even out to backward angles except for  $^{50}\text{Cr}$ , OM Set III. For these optimum calculations, the OM parameters of Set III as listed in Table I were used for both the  $^3\text{He}$  and  $t$  channels for  $^{62}\text{Ni}$  and  $^{90}\text{Zr}$ , but for  $^{50}\text{Cr}$  the strength of the imaginary triton well needed to be increased to 50 MeV for

a good fit. For Set IV the imaginary part of the triton optical potential needed to be modified by either an increase in  $r_I$  ( $r_I=1.60$  fm for  $^{90}\text{Zr}$ ) or  $W_V$  ( $W_V=40$  MeV for  $^{62}\text{Ni}$  and  $W_V=60$  MeV for  $^{50}\text{Cr}$ ). The other two OM sets failed to fit the data at 70 MeV even with large changes in the triton OM parameters, although Set I did provide an acceptable fit to the 37.5-MeV data. (Variations in the range of the Yukawa interaction from 0.7 to 1.4 fm did little to change the over-all structure, although there were changes in the heights of the maxima. OM Set III had a preference for  $\mu=1.0$ , although this was not clear for the other sets.)

From the microscopic calculations, some conclusions can be drawn regarding OM parameters, as the form factors for a particular reaction are now the same for all sets. In  $^3\text{He}$  elastic scattering analyses ambiguities have been noted in both

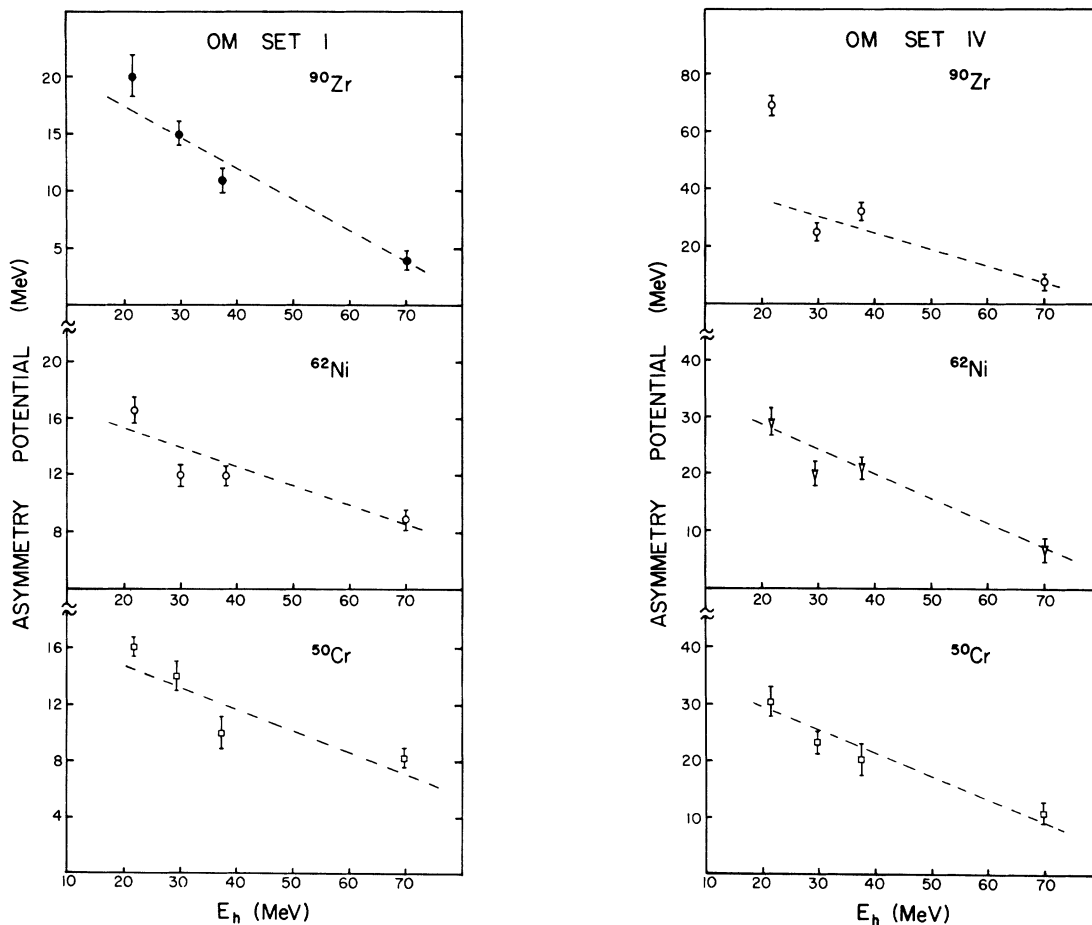


FIG. 5. Strength of the asymmetry potential  $U_1$  extracted from the present 70-MeV ( $^3\text{He}, t$ ) data on  $^{62}\text{Ni}$ ,  $^{90}\text{Zr}$ , and  $^{50}\text{Cr}$  and that of Ref. 6 at 37.5, 29.7, and 21.4 MeV for calculations with a macroscopic form factor (with shapes as described in the text but the same at each energy) for OM Sets I and IV. The dashed lines are only to guide the eye. The error bars correspond to about a 10% uncertainty in the extraction of  $U_1$  due to statistical errors in the data and judgments in the normalization between theory and experiment.

the size of the real potential (family) or in the form of the imaginary term. Recent studies<sup>13, 14</sup> indicate a potential family of 120 MeV ( $r_0 = 1.1$  fm) and a surface-peaked imaginary term best describe the  $^3\text{He}$  elastic scattering data especially when large-angle scattering data is included. Different sets of OM parameters generated in fitting 70-MeV  $^3\text{He}$  elastic data on  $^{50}\text{Ti}$  and  $^{51}\text{V}$ <sup>11</sup> are listed in Table II. These cover the 110- and 170-MeV potential families with a volume or a surface-peaked form for the imaginary term. Microscopic DWBA calculations for the reaction  $^{62}\text{Ni}(^3\text{He}, t)-^{62}\text{Cu}(\text{IAS})$  were carried out with these OM parameters and are shown in Fig. 4. It is seen that a volume imaginary term (and not a surface-peaked term) is required. (It was previously noted that OM Set II provided no fits in microscopic calculations to any of the data.) It is also seen that the family of parameters with a real potential of 110–120 MeV does a better job than the set of 160–170 MeV. The fits in Fig. 3 are also in general better for Set III than for Set IV for these microscopic calculations. [The Set IV family of parameters

is in the same family ( $VR^2$ ) as the 160–170-MeV potentials.]

#### IV. INTERACTION STRENGTHS

The strength of the asymmetry potential  $U_1(r)$  and the projectile-nucleon interaction  $V_\tau$  were obtained by a normalization between the data and DWBA calculations. For the macroscopic calculations the asymmetry potential strength  $U_1$  is essentially equal to  $W$  of Eq. (2), as the bulk of the calculated cross section arises from the imaginary part of the interaction term. These strengths were extracted in two ways: by normalization between the data and theory at the first maximum in the angular distributions [ $V_1(1\text{st Max})$ ], and by normalization between the integrated experimental and theoretical cross sections, accounting for our finite solid angle in the latter summation ( $V_{\text{TOT}}$ ). Both methods gave similar answers. The values of  $U_1$  for  $^3\text{He}$  bombarding energies of 70, 37.5, 29.7, and 21.4 MeV for our macroscopic calculations are shown in Fig. 5 for OM Sets I and

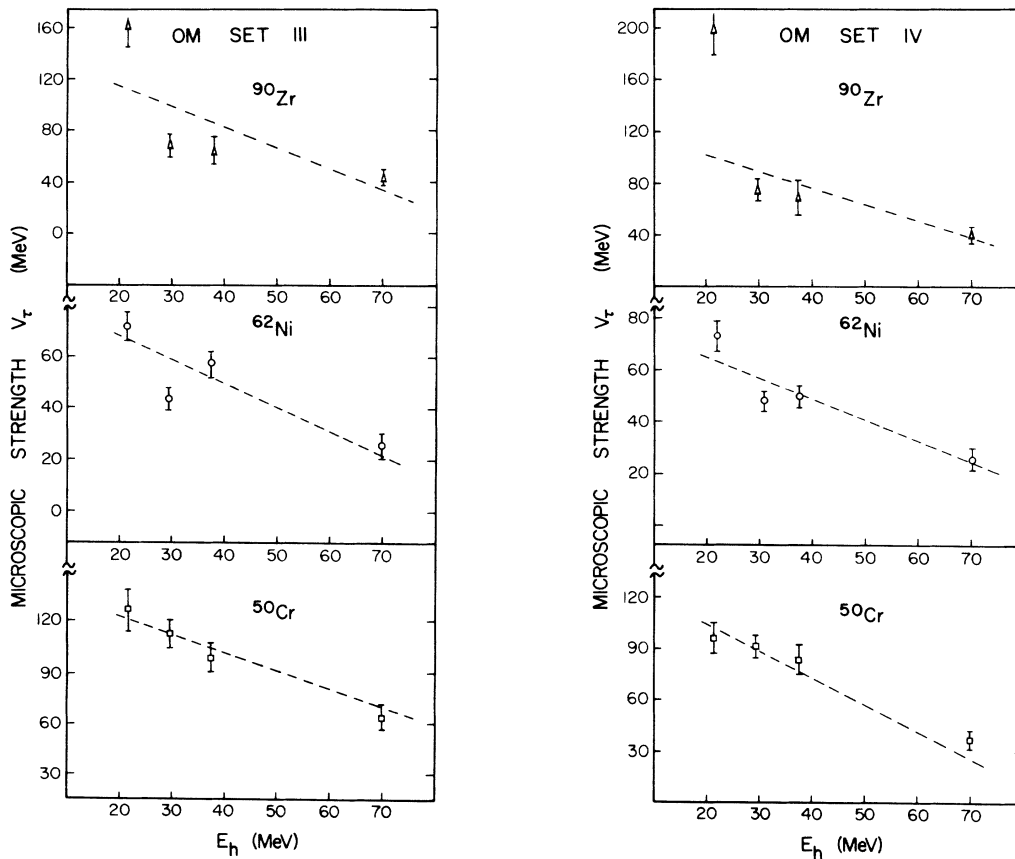


FIG. 6. Strength of the microscopic interaction  $V_\tau$  as a function of  $^3\text{He}$  bombarding energy for OM Sets III and IV. See caption for Fig. 5.

TABLE III. Interaction strengths. Values of  $V_\tau$  and  $U_1$  (in MeV) obtained with two different types of normalization between experiment and theory (see text) as a function of OM set used. The numbers in parenthesis for each OM set correspond to the relative strengths of real and imaginary terms in the macroscopic form factor. The OM parameters for each set are those listed in Table I with the footnoted exceptions being those changes required in the triton parameters or form-factor geometry at 70 MeV for a good fit.

OM Set	$V_{\text{tot}}$		$V_1$ (1st Max)	
	70 MeV	37.5 MeV	70 MeV	37.5 MeV
$^{62}\text{Ni}$				
I ( $V=W$ )	8.4	13.3	4.9	12.4
II ( $V=5W^a$ )	8.9	17	9.4	17
IV ( $V=W$ )	10	22	6.8	21
III (Micro)	24	51	25	54
IV (Micro <sup>b</sup> )	16	55	27	52
$^{90}\text{Zr}$				
I ( $V=9W$ )	3.5	13	3.7	11
II ( $V=3W^c$ )	4.8	18	4.5	14
IV ( $V=2W$ )	7.9	41	7.8	32
III (Micro)	46	105	45	70
IV (Micro <sup>d</sup> )	38	91	40	69

<sup>a</sup>  $r_f = 1.46$  fm for form factor.

<sup>b</sup>  $W_V = 40$  MeV for triton OM.

<sup>c</sup>  $r_f = 1.40$  fm for form factor.

<sup>d</sup>  $r_f = 1.60$  fm,  $W_V = 15$  MeV for triton OM.

IV where the lower-energy data of Fadner, Kraushaar, and Hayakawa<sup>6</sup> has been reanalyzed in the same way. (Only in Set IV is there an energy dependence in the OM parameters.) For both OM sets and for all three nuclei,  $^{62}\text{Ni}$ ,  $^{90}\text{Zr}$ , and  $^{50}\text{Cr}$ , there is a marked decrease in the strength of the asymmetry term as a function of  $^3\text{He}$  bombarding energy. Our results at 70 MeV are consistent with the trend seen at lower energies. The magnitude of the asymmetry term (or  $W$ ) at 70 MeV has the average values of 7, 6, and 9 MeV for  $^{62}\text{Ni}$ ,  $^{90}\text{Zr}$ , and  $^{50}\text{Cr}$ , respectively. [Note the factor of 4 in Eq. (2).] These numbers are in general a factor of 2 or 3 smaller than those found in other

( $^3\text{He}, t$ ) work<sup>3,4,15</sup> (at lower bombarding energies however).

The values of  $V_\tau$  for our microscopic calculations as a function of  $^3\text{He}$  energy are shown in Fig. 6 for OM Sets III and IV. Again the data of Fadner, Kraushaar, and Hayakawa has been reanalyzed with these OM sets, checking each time for a reasonable fit to the data. (A Yukawa interaction of range 1.0 fm was used.) For all three nuclei considered the trend again shows a decrease in the value of the isospin-dependent interaction term as a function of bombarding energy. The rate of change of  $V_\tau$  with energy is of the same order as that for the energy dependence of the asymmetry strength in the macroscopic calculations. Our results at 70 MeV for the microscopic strengths have the average values for OM Sets III and IV of 26, 42, and 50 MeV for  $^{62}\text{Ni}$ ,  $^{90}\text{Zr}$ , and  $^{50}\text{Cr}$ , respectively. Numbers found in other ( $^3\text{He}, t$ ) work (outside of Ref. 6) are between 30 and 90 MeV (for a range of 1 fm). The effective  $^3\text{He}$ -nucleon interaction strength can be expressed in terms of the nucleon-nucleon strength by the relationship of Wesolowski *et al.*,<sup>3</sup>  $V_\tau = V_{n-n} e^{\alpha^2/4}$ , where  $\alpha$  is the inverse range. This yields an average value of  $V_{n-n} = 15$  MeV for  $^{62}\text{Ni}$  at 70 MeV, in comparison with values of 10–20 MeV found for ( $p, n$ ) studies<sup>2,16</sup> at bombarding energies between 15 and 30 MeV.

Our results for the ( $^3\text{He}$ -nucleon) interaction strengths found at 70 MeV are summarized in Table III as a function of the OM set used (for best fit) for  $^{62}\text{Ni}$  and  $^{90}\text{Zr}$ . Values from the two normalization methods used in extracting these strengths are tabulated, as well as results of our reanalysis of the 37.5-MeV data. These results again point out the decrease in the charge-exchange interaction strength at 70 MeV, relatively independent of the OM set used in the analysis.

## V. SUMMARY

A study of ( $^3\text{He}, t$ ) transitions at 70 MeV to IAS of  $^{62}\text{Ni}$ ,  $^{90}\text{Zr}$ , and  $^{50}\text{Cr}$  has reached the following conclusions: (i) The interaction strengths extract-

TABLE IV. Interaction strengths; summary.

Source	Targets	Particle and energies (MeV)	% decrease in $V_\tau$ /MeV particle energy
Present MSU & Fadner (Ref. 6)	Ni, Zr Cr	$^3\text{He}$ , 21–70	1–2
Galonsky <sup>a</sup>	Al, Zr, V	$p$ , 22–40	$1\frac{1}{2}$ –2
Becchetti (Ref. 5)	Ni	$^3\text{He}$ , 25–37	$2\frac{1}{2}$
Clough (Ref. 16)	$1p$ shell	$p$ , 30–50	3
Wong (Ref. 2)	Al–Pb	$p$ , 17–50	$1\frac{1}{2}$

<sup>a</sup> A. Galonsky, R. K. Jolly, R. St. Onge, and T. Amos, to be published.

ed from both microscopic (shell-model) and macroscopic (generalized optical-model) calculations are approximately 50% smaller than at lower bombarding energies and dramatize the trend of the energy dependence of the isospin-dependent potential seen there; (ii) the shape of the form factor in the macroscopic calculations is different for each of the three nuclei, but consistent with lower energy findings; (iii) in the microscopic analyses, only those calculations with optical-model parameters that had a volume imaginary term fitted the data. The first two conclusions in general are independent of the OM sets that are used, although the magnitude of the interaction strength and the shape of the macroscopic form factors are quite dependent upon the OM parameters.

We can relate the conclusions concerning the

energy dependence of the interaction strengths to other work, including ( $p, n$ ) reactions; we summarize some of these findings in Table IV, for those results in which IAS transitions were either investigated or analyzed over a range of bombarding energies. The percent decrease in the interaction strength  $V_\tau$  per MeV of incident particle energy is seen to average about  $(2 \pm 1)\%$  for all cases, including the present results. This number is significantly larger than the energy-dependent decrease in the real part of the  ${}^3\text{He}$ -nucleus optical potential. These results should provide additional impetus for studies into the DWBA with respect to charge-exchange reactions; two-step processes and exchange might be important in describing these energy-dependent effects.

---

†Work supported by the National Science Foundation.

<sup>1</sup>G. R. Satchler, R. M. Drisko, and R. H. Bassel, *Phys. Rev.* **136**, B637 (1964).

<sup>2</sup>C. Wong, J. D. Anderson, J. W. McClure, B. A. Pohl, and J. J. Wesolowski, *Phys. Rev. C* **5**, 158 (1972).

<sup>3</sup>J. J. Wesolowski, E. H. Schwarz, P. G. Roos, and C. A. Ludeman, *Phys. Rev.* **169**, 878 (1968).

<sup>4</sup>P. Kossanyi-Demay, P. Roussel, H. Faraggi, and R. Schaeffer, *Nucl. Phys.* **A148**, 181 (1970).

<sup>5</sup>F. D. Becchetti, W. Makofske, and G. W. Greenlees, to be published.

<sup>6</sup>W. L. Fadner, J. J. Kraushaar, and S. I. Hayakawa, *Phys. Rev. C* **5**, 859 (1972).

<sup>7</sup>G. C. Ball and J. Cerney, *Phys. Rev.* **177**, 1466 (1969); and D. C. Hensley, C. D. Goodman, and M. J. Saltmarsh, ORNL Report No. ORNL-4649, 1970 (unpublished).

<sup>8</sup>Computer code by P. D. Kunz.

<sup>9</sup>F. D. Becchetti and G. W. Greenlees, in *Polarization Phenomena in Nuclear Reactions*, edited by H. H. Barschall and W. Haerberli (Univ. of Wisconsin Press, Madison, 1971), p. 682.

<sup>10</sup>E. F. Gibson, B. W. Ridley, J. J. Kraushaar, M. E. Rickey, and R. H. Bassel, *Phys. Rev.* **155**, 1194 (1967).

<sup>11</sup>R. A. Hinrichs, R. R. Doering, and A. Galonsky, *Bull. Am. Phys. Soc.* **16**, 628 (1971); and to be published.

<sup>12</sup>C. B. Fulmer, private communication.

<sup>13</sup>C. B. Fulmer and J. C. Hafele, to be published.

<sup>14</sup>G. R. Siegel, F. B. Shull, and J. C. Hafele, *Bull. Am. Phys. Soc.* **16**, 646 (1971).

<sup>15</sup>W. L. Fadner, J. J. Kraushaar, and L. C. Farwell, *Nucl. Phys.* **A178**, 385 (1971).

<sup>16</sup>A. S. Clough, C. J. Batty, B. E. Bonner, and L. E. Williams, *Nucl. Phys.* **A143**, 385 (1970).